2018 European Control Conference (ECC)
June 12-15, 2018. Limassol, Cyprus

Multirobot Target Enclosing with Freely Selected Observation Distances

Miguel Aranda and Youcef Mezouar

Abstract— **Tasks such as surveillance, escorting or robotic object interaction benefit from having complete and detailed perception of a target entity, provided by multiple mobile sensors. The ensuing challenge of suitably coordinating the sensor motions for such collective observation is addressed in this paper. In particular, we consider a moving target in 3D space, and focus on achieving prescribed relative viewing angles, which we encapsulate by a default desired enclosing pattern, with respect to this target. The paper contributes a novel control method that makes a team of mobile agents converge to the desired configuration of viewpoints with respect to a point that tracks the target. Relative agent position regulation and target tracking are integrated via a formation-based controller relying on global information that incorporates an optimal pattern rotation. We also introduce flexibility in the team geometry, allowing each agent to select freely, without knowledge of the others, its desired distance to the target. This can allow to, e.g., optimize perception quality and avoid collisions. Notably, we show that even with these distributed adjustments, the team motions remain steady, which contributes to obtaining stable perception and efficient control performance. In addition, each robot can operate on its independent local reference frame. Simulation tests illustrate the presented methodology.**

I. Introduction

Increasing the presence of robots in industrial, agricultural, medical or domestic environments is widely regarded as fundamental for the improvement of work conditions and societal advancement. This calls for robots capable of complex behaviors in dynamic scenarios, which requires versatility and adaptability. In this context, a team of multiple agents including cooperative robots, and possibly human agents as well, can provide notable advantages such as increased abilities and higher efficiency and reliability.

The specific task of observing a target, which we address here, benefits from having different viewpoints provided by multiple sensors placed at diverse positions; this can avoid occlusions and improve the quality of perception via data integration (e.g., position triangulation). Such observation capabilities allow to generate a suitable model of an object to be manipulated or transported by a robotic system. They can also find use in surveillance and escorting problems. In particular, a diversity of viewing angles is a requirement in, for instance, motion capture systems [1] which are, however, restricted to a fixed environment with a static setup of sensors. It becomes interesting, for the application scenarios mentioned, to extend the concept to mobile targets in dynamic environments; this can be achieved using robot-mounted sensors, where the robots must move to concurrently perceive the target and track its motion [2].

A key goal within this problem is to define team configurations and motion policies that optimize the quality of collective perception by, e.g., uncertainty minimization, as studied in [3]–[7]. However, a fundamental concurrent goal is also to suitably control the interagent states during task execution; the robots must preserve relative positions that allow them to perceive and/or communicate with each other and avoid collisions. These considerations connect with the extensive field of multiagent formation control, which deals with attaining and maintaining team configurations prescribed generally by distances and/or angles [8]–[14]. Standard methods to control formations focus on managing the agents' relative states, and are not oriented towards providing collective perception and tracking of a target, as in this paper. Formation-based schemes have been used within target observation tasks [15], [16], with lower dimensionality and adaptability of the team shape compared to our method. Strategies based on persistent motion –i.e., target encirclement– in other related work [17]–[19] do not allow steady agent motions, which are interesting for efficiency and increased stability of perception data. Our method integrates the two goals mentioned above, providing suitable perception diversity and controlling the team agents' relative states. This is done by prescribing a default target-enclosing formation, and driving the robots to achieve an optimal –in terms of a global shape alignment metric– rotated version of that formation, while tracking the target's motion.

We introduce flexibility in the formation shape –to, e.g., avoid collisions, adapt to the target's size, or improve perception quality– by allowing free selection by each individual robot of its desired distance to the target. Still, the pursued perceptual diversity is achieved, as the agents' relative positions evolve towards a pattern in which they maintain the same relative target-viewing angles as in the default formation. It is shown via the study of the pattern rotation dynamics that the formation and target tracking behaviors remain stable and steady, independently from the distributed distance selection procedure used. In addition, the method we present applies to general 3D motions and can be implemented using local measurements with no common reference frames, which is known to make coordination more complex to study [8] but provides great flexibility and simplicity advantages. The work in [20] is the basis for the method we propose. Contrary to that previous paper, here the target is mobile, and the desired distances to the target are not fixed and can be selected independently by each agent.

The authors are with SIGMA Clermont, Institut Pascal, Université Clermont Auvergne, Clermont-Ferrand, France. {miguel.aranda, youcef.mezouar}@sigma-clermont.fr

This work was supported by the French Government via FUI program (project Aerostrip) and Investissements d'avenir program (I-SITE project CAP 20-25).

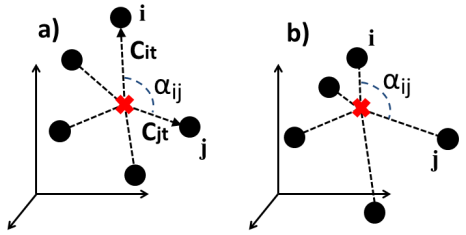

Fig. 1. a) Default formation of agents (circles) enclosing a target (cross) in 3D space. b) Formation preserving the relative viewing angles α_{ij} with respect to the target in a), while having different agent-target instances. Note that if a given rotation is applied to every vector between the target and an agent, the relative angles α_{ij} for all pairs of agents are preserved.

II. Problem Definition

Consider a group of $N > 2$ robots modelled as point masses in $\mathbb{R}^3$. Each robot is identified by an index $i \in \{1, ..., N\}$ and its dynamics can be expressed through a single integrator model, i.e., it satisfies:

$$\dot{\mathbf{q}}_\mathbf{i} = \mathbf{u}_\mathbf{i}, \tag{1}$$

where $\mathbf{q_i} \in \mathbb{R}^3$ is the position of robot i and $\mathbf{u_i} \in \mathbb{R}^3$ its control input. We further define $\mathbf{q_t} \in \mathbb{R}^3$ as the position of the *target*. The robots have to collectively observe this target, which moves with finite-norm arbitrary velocity $\mathbf{v_t}$:

$$\dot{\mathbf{q}}_\mathbf{t} = \mathbf{v_t}. \tag{2}$$

The robots' and target positions are expressed in an arbitrary global reference frame. We use the following notation to refer to relative position vectors: $\mathbf{q_{ij}} = \mathbf{q_i} - \mathbf{q_j} = -\mathbf{q_{ji}}$.

The problem we address can be stated as ensuring that the target is observed from a suitable diversity of viewpoints throughout its movement. The framework described next gives the precise definition of the problem. We define the *default desired configuration* as a reference layout of the N robots in their configuration space. This is encapsulated via relative position vectors, being $\mathbf{c_{ji}} \in \mathbb{R}^3$, $\forall i, j \in \{1, ..., N\}$, the vector from robot i to robot j. In addition, we denote as $\mathbf{c_{ti}}$ the desired vector from robot i to the target. As we want to enclose the target, we assume its desired position is in the centroid of the desired pattern. Thus, $\sum_{i=1}^{N} \mathbf{c_{ti}} = \mathbf{0}$. For controller analysis purposes, we assume the desired geometry is generic [11] and without exact symmetries. Note that this is not restrictive, as by infinitesimal modifications one can ensure the condition holds for any desired geometry.

From this geometric description, we can directly define an associated angle-based configuration, specified by the relative angles at which pairs of robots observe the target. In particular, for any pair $i, j \in \{1, ..., N\}$, we define their desired relative viewing angle with respect to the target as $\alpha_{\mathbf{ij}} = \angle(\mathbf{c_{it}}, \mathbf{c_{jt}})$. Thus, a way to encode a given desired target-observation diversity is by prescribing an appropriate default enclosing formation, which directly encapsulates the desired relative target-viewing angles. An illustration of the default formation definition appears in Fig. 1.

Then, we consider that the control goal is achieved if there exist a point $\mathbf{p_a} \in \mathbb{R}^3$, a rotation matrix $\mathbf{R_a} \in SO(3)$, and a set of N scalar parameters $s_{ai} > 0$ such that:

$$\mathbf{q_i} = \mathbf{p_a} + \mathbf{R_a} \mathbf{c_{it}^{s_{ai}}}, \quad \forall i \in \{1, ..., N\}, \tag{3}$$

where $\mathbf{c_{it}^{s_{ai}}} = s_{ai}\mathbf{c_{it}}$, and if simultaneously $\mathbf{p_a}$ remains suitably close to $\mathbf{q_t}$.

We see next that the condition (3) implies the desired relative target-viewing angles are achieved with respect to $\mathbf{p_a}$. For this to occur, the angle –which we denote as β_{ij}– between a pair of vectors $\mathbf{q_i} - \mathbf{p_a}$ and $\mathbf{q_j} - \mathbf{p_a}$ must equal α_{ij}, $\forall i, j$. Let us rotate all these vectors by the common matrix $\mathbf{R_a}^{-1}$, which clearly does not change the angles between them, obtaining a set of vectors defined as follows: $\mathbf{v_i} = \mathbf{R_a}^{-1}(\mathbf{q_i} - \mathbf{p_a}) = \mathbf{c_{it}^{s_{ai}}}$ $\forall i$. Then for each i, the angle between $\mathbf{v_i}$ and $\mathbf{c_{it}}$, denoted as β_{vci}, is zero, since $\cos(\beta_{vci}) = < \mathbf{v_i}, \mathbf{c_{it}} > /(||\mathbf{v_i}|| \cdot ||\mathbf{c_{it}}||) = s_{ai} < \mathbf{c_{it}}, \mathbf{c_{it}} > /(s_{ai}(||\mathbf{c_{it}}|| \cdot ||\mathbf{c_{it}}||)) = 1$. Hence, $\beta_{ij} = \alpha_{ij}$, $\forall i, j$.

As said above, the default desired configuration captures the relative angular constraints that define our problem. Its usefulness also lies in that it can represent a pattern that, in the absence of other task constraints, is the preferred configuration of the team due to advantages such as facilitation of agent interactions, favorable geometry and size, and/or safety. The agents can nonetheless deform the shape of the default configuration –as explained in subsequent sections– to provide observation and navigation flexibility, while still satisfying the relative angular constraints.

III. Control Strategy

This section describes the proposed multirobot control strategy to carry out the task of target enclosing for observation according to the definition established in the preceding section. Some of the contents are similar to those in [20] although a different control strategy is proposed here. A suitable manner to solve the problem is by making the agents move towards an objective relative multiagent pattern that satisfies the condition in (3). Note that a common rotation of all desired target-agent vectors preserves the angles α_{ij}. Therefore, it is interesting to move the agents towards an *optimally* rotated version of the default formation, as this can increase the efficiency of their motions. To do so, we define the rotation by solving an optimal alignment problem between two *shapes*: the sets of current and desired points. We can express a cost function for this alignment as the following sum of quadratic distances:

$$\gamma = \sum_i \sum_j ||\mathbf{q_{ij}} - \mathbf{R_c}\mathbf{c_{ij}}||^2, \tag{4}$$

where i, j both go from 1 to N, and $\mathbf{R_c} \in SO(3)$ is a rotation matrix acting on the desired vectors. It can be seen that this cost function is equivalent to the one considered in orthogonal Procrustes shape fitting problems [21].

A. Computation of the rotation matrix

The rotation matrix is a fundamental element of the control method we present, as it enables the goals of optimality – it minimizes γ– and independence of a global coordinate

system, as shown later. By stacking the interagent position vectors, we obtain the following $N^2 \times 3$ matrices:

$$\mathbf{Q} = [\mathbf{q_{11}}...\mathbf{q_{1N}}\ \mathbf{q_{21}}...\mathbf{q_{2N}}...\mathbf{q_{N1}}...\mathbf{q_{NN}}]^T$$
$$\mathbf{C} = [\mathbf{c_{11}}...\mathbf{c_{1N}}\ \mathbf{c_{21}}...\mathbf{c_{2N}}...\mathbf{c_{N1}}...\mathbf{c_{NN}}]^T. \quad (5)$$

We define the matrix $\mathbf{A} = \mathbf{C}^T\mathbf{Q}$ from the two sets. We want to find $\mathbf{R}$ such that choosing $\mathbf{R_c} = \mathbf{R}$ in (4) makes γ minimum for given matrices $\mathbf{Q}$ and $\mathbf{C}$. This rotation can be computed by the Kabsch algorithm [22], using the Singular Value Decomposition (SVD) of $\mathbf{A}$, $\mathbf{A} = \mathbf{U\Lambda V}^T$, as follows:

$$\mathbf{R} = \mathbf{VDU}^T = \mathbf{V}\begin{pmatrix} 1 & 0 & 0 \\ 0 & 1 & 0 \\ 0 & 0 & d \end{pmatrix}\mathbf{U}^T, \quad (6)$$

where $d = sign(det(\mathbf{VU}^T))$. The solution for $\mathbf{R}$ is unique with this algorithm unless $rank(\mathbf{A}) < 2$ or the smallest singular value of $\mathbf{A}$ is degenerate [23]. This uniqueness will be ensured by the conditions provided in our stability analysis. Each agent computes this rotation matrix, which is common to all of them, and uses it to define its control law.

B. Free individual selection of desired agent-target distances

We propose to allow each agent to select independently its desired distance to the target. This is an appealing capability as it can allow to, e.g., optimize target perception quality or avoid collisions during navigation. Specifically, agent i will want to situate itself at a desired distance from the target equal to $||\mathbf{c^s_{ti}}|| = s_i||\mathbf{c_{ti}}||$, where $s_i > 0$ is a bounded constant factor, which we call the *control scale* of i, and which is chosen freely by i and unknown to all other agents.

C. Control law

Every agent $i \in \{1, ..., N\}$ determines its motion command via the following closed-loop control law:

$$\mathbf{u_i} = \dot{\mathbf{q}}_\mathbf{i} = K_c(\mathbf{q_{ti}} - \mathbf{Rc^s_{ti}}), \quad (7)$$

where K_c is a positive control gain and $\mathbf{c^s_{ti}} = s_i\mathbf{c_{ti}}$ represents $i's$ desired position vector to the target, weighted by its control scale. With this law, the agent moves towards a position situated at its desired distance to the target, while also taking into account the team coordination goal via $\mathbf{R}$ (6), which is computed by i at each time instant.

D. Implementation details and reference frames

To compute (7), a robot i needs to know the relative positions of the other agents with respect to itself, $\mathbf{q_{ji}}\ \forall j \neq i$. Thus, since $\mathbf{q_{jk}} = \mathbf{q_{ji}} - \mathbf{q_{ki}}$, i clearly can compute the matrix $\mathbf{Q}$ (5) and then $\mathbf{R}$ (6). This required relative position information can be obtained by the robot via sensing, or by integrating data received from the other robots –via communications– with its own measurements. We note that the robots need global information of the team; we deem this to be a reasonable requirement, as the number of agents for a cooperative target perception task will remain small in typical practical scenarios. Thus, the data processing load will be low. Employing a central unit of computation would increase the efficiency of processing, albeit creating a central point of failure and making the use of communications mandatory. Agent i also needs to perceive the target and its relative position, $\mathbf{q_{ti}}$. The sensing of the target, on which we do not elaborate here, can be done with a special dedicated sensor.

A fundamental aspect to note is that this control can be computed if each robot uses a local and arbitrarily oriented coordinate frame. Let us illustrate this for an agent k. Observe first that $\mathbf{q_{tk}}$ and $\mathbf{q_{jk}}$, $\forall j \in \{1, ..., N\}$, are *relative* measurements, and therefore, there is no need for a common coordinate origin for the robots. Furthermore, the specific orientation of each robot's reference frame is irrelevant. To see this, let us denote as $\mathbf{P_k} \in SO(3)$ the relative rotation matrix between the global frame and the local frame in which k operates, i.e., $\mathbf{q^P_k} = \mathbf{P_k q_k}$, with $\mathbf{q^P_k}$ being the position of k in a frame centered in the global origin and aligned with the local frame. We next look at (4), and assume given fixed positions $\mathbf{q_i}$. Let us denote with a superscript Lk the variables expressed in $k's$ local frame, and write down the cost function (note that $\mathbf{q^{Lk}_{ij}} = \mathbf{P_k q_{ij}}$):

$$\gamma^{Lk}(\mathbf{R^{Lk}_c}) = \sum_i \sum_j ||\mathbf{q^{Lk}_{ij}} - \mathbf{R^{Lk}_c c_{ij}}||^2 =$$
$$= \sum_i \sum_j ||\mathbf{q_{ij}} - \mathbf{P_k^{-1} R^{Lk}_c c_{ij}}||^2 = \gamma(\mathbf{P_k^{-1} R^{Lk}_c}), \quad (8)$$

for any $\mathbf{R^{Lk}_c} \in SO(3)$. Thus, clearly, the unique optimal rotations in the two frames must satisfy $\mathbf{R} = \mathbf{P_k^{-1} R^{Lk}}$, i.e., $\mathbf{R^{Lk}} = \mathbf{P_k R}$. Then, the same motion is obtained when computing the control in each of the two frames, since:

$$\mathbf{u^{Lk}_k} = K_c(\mathbf{P_k q_{tk}} - \mathbf{P_k R c^s_{tk}}) = \mathbf{P_k u_k}. \quad (9)$$

IV. Stability analysis

We study next the stability properties of the target enclosing strategy. The analysis uses the following assumption.

A1: $rank(\mathbf{A}) > 1$ and the smallest singular value of $\mathbf{A}$ is nondegenerate at every time instant.

Let us explain this assumption. When there are multiple solutions for $\mathbf{R}$ (see Section III-A), this rotation is not differentiable with respect to time, which is a requisite of our stability analysis presented below. The scenarios where this situation can arise, expressed by rank and SVD conditions on matrix $\mathbf{A}$, are associated with perfect symmetries or singular geometries of the current and desired relative robot positions. These configurations have zero measure, meaning that an infinitesimal perturbation of the robot positions takes $\mathbf{A}$ out of them. In addition, as will be shown, they are unrelated with the control strategy proposed (i.e., the controller does not move the system towards them). Then, as they do not represent an issue in reality, we disregard them –by using A1– in the stability analysis that follows. Further discussion on this matter is provided in Remark 1.

Theorem 1: Under the controller (7) and provided that assumption A1 is satisfied, the rotation matrix $\mathbf{R}$ remains constant for all time.

Proof: Let us start by writing down the interagent dynamics, from (7), as follows:

$$\dot{\mathbf{q}}_\mathbf{ij} = \dot{\mathbf{q}}_\mathbf{i} - \dot{\mathbf{q}}_\mathbf{j} = -K_c(\mathbf{q_{ij}} - \mathbf{R}(\mathbf{c^s_{it}} - \mathbf{c^s_{jt}})). \quad (10)$$

We define a constant $N^2 \times 3$ matrix $\mathbf{C_s} = [\mathbf{c^s_{1t}} - \mathbf{c^s_{1t}}\ \ \mathbf{c^s_{1t}} - \mathbf{c^s_{2t}}\ \ ...\ \ \mathbf{c^s_{Nt}} - \mathbf{c^s_{Nt}}]^T$. One can then provide this expression for the dynamics of $\mathbf{Q}$ (5):

$$\dot{\mathbf{Q}}(t) = -K_c[\mathbf{Q} - \mathbf{C_s}\mathbf{R}^T]. \tag{11}$$

The dynamics of $\mathbf{A}$ has, therefore, the following form:

$$\dot{\mathbf{A}} = \mathbf{C}^T\dot{\mathbf{Q}} = -K_c(\mathbf{A} - \mathbf{C}^T\mathbf{C_s}\mathbf{R}^T). \tag{12}$$

We will study the evolution of $\mathbf{R}$ by studying the evolution of $\mathbf{A}$. Notice that it is immediate from the definitions of $\mathbf{A}$ and $\mathbf{R}$ (Section III-A) that $\mathbf{AR}$ is a symmetric matrix, so:

$$\mathbf{R}^T\mathbf{A}^T - \mathbf{AR} = \mathbf{0}, \tag{13}$$

and in consequence:

$$\dot{\mathbf{R}}^T\mathbf{A}^T + \mathbf{R}^T\dot{\mathbf{A}}^T - \dot{\mathbf{A}}\mathbf{R} - \mathbf{A}\dot{\mathbf{R}} = \mathbf{0}. \tag{14}$$

We can now substitute (12) in this last equation and get:

$$\begin{aligned}\dot{\mathbf{R}}^T\mathbf{A}^T - K_c\mathbf{R}^T\mathbf{A}^T + K_c\mathbf{R}^T\mathbf{R}{\mathbf{C_s}}^T\mathbf{C}\\ +K_c\mathbf{AR} - K_c\mathbf{C}^T\mathbf{C_s}\mathbf{R}^T\mathbf{R} - \mathbf{A}\dot{\mathbf{R}} = \mathbf{0}.\end{aligned} \tag{15}$$

Symmetry of $\mathbf{AR}$ allows one to write:

$$\dot{\mathbf{R}}^T\mathbf{A}^T - \mathbf{A}\dot{\mathbf{R}} + K_c({\mathbf{C_s}}^T\mathbf{C} - \mathbf{C}^T\mathbf{C_s}) = \mathbf{0}. \tag{16}$$

Let us now define and examine $\mathbf{P_c} = {\mathbf{C_s}}^T\mathbf{C}$. By expressing $\mathbf{C_s} = \mathbf{C_{s1}} - \mathbf{C_{s2}}$ and, from (5), $\mathbf{C} = \mathbf{C_1} - \mathbf{C_2}$, where $\mathbf{C_{s1}} = [\mathbf{c^s_{1t}}\ ...\ \mathbf{c^s_{1t}}\ \mathbf{c^s_{2t}}\ ...\ \mathbf{c^s_{2t}}\ ...\ \mathbf{c^s_{Nt}}]^T$ and $\mathbf{C_{s2}} = [\mathbf{c^s_{1t}}\ ...\ \mathbf{c^s_{Nt}}\ \mathbf{c^s_{1t}}\ ...\ \mathbf{c^s_{Nt}}\ ...\ \mathbf{c^s_{Nt}}]^T$ –analogous expressions without the s superscripts clearly apply to $\mathbf{C_1}$ and $\mathbf{C_2}$–, an individual element of $\mathbf{P_c}$ can be seen to be equal to:

$$\begin{aligned}\mathbf{P_c}[i,j] = &\sum_{k=1}^{N^2}\mathbf{C_{s1}}[k,i]\mathbf{C_1}[k,j] + \mathbf{C_{s2}}[k,i]\mathbf{C_2}[k,j]\\ &- \mathbf{C_{s1}}[k,i]\mathbf{C_2}[k,j] - \mathbf{C_{s2}}[k,i]\mathbf{C_1}[k,j],\end{aligned} \tag{17}$$

for $i,j = 1,2,3$. The structure of the matrices allows to write: $\sum_{k=1}^{N^2}\mathbf{C_{s1}}[k,i]\mathbf{C_2}[k,j] = \sum_{k=1}^{N}\mathbf{c^s_{kt}}[i]\sum_{l=1}^{N}\mathbf{c_{lt}}[j] = 0$, since every sum along a given coordinate (x, y or z) of the N vectors from the target ($\mathbf{c_{lt}}$) is zero. We note again that this is so because the target is at the centroid of the default desired configuration. Similarly, the last sum of terms in (17) can also be seen to be zero. Hence, only the two sums in the first line of (17) are nonzero, and one has:

$$\begin{aligned}\mathbf{P_c}[i,j] &= \sum_{k=1}^{N^2}\mathbf{C_{s1}}[k,i]\mathbf{C_1}[k,j] + \mathbf{C_{s2}}[k,i]\mathbf{C_2}[k,j]\\ &= \sum_{k=1}^{N^2}s_{p1}(k)\mathbf{C_1}[k,i]\mathbf{C_1}[k,j] + s_{p2}(k)\mathbf{C_2}[k,i]\mathbf{C_2}[k,j],\end{aligned} \tag{18}$$

where $s_{p1}(k)$ and $s_{p2}(k)$ are scale values that depend only on the index k. From (18), it is clear that $\mathbf{P_c}$ is a symmetric matrix. Then, (16) becomes:

$$\dot{\mathbf{R}}^T\mathbf{A}^T - \mathbf{A}\dot{\mathbf{R}} = \mathbf{0}. \tag{19}$$

We refer at this point to the analysis of the solutions of an identical equation in [20, Prop. 1]. Using the properties of the time-derivative of the rotation matrix and the SVD of $\mathbf{A}$, and under assumption A1, one can see that indeed the correct solution to (19) is $\dot{\mathbf{R}} = \mathbf{0}$. Thus, the rotation matrix remains constant for all time when using the proposed controller. ■

Let us stress the significance of this result. The control scales s_i very directly determine the directions of motion – see (7)– and are chosen freely without coordination among agents. Thus, even though they are not used in the computation of $\mathbf{R}$, one could expect the time-evolution of $\mathbf{R}$ to depend on the values of these scales. To the contrary, the analysis has shown that $\mathbf{R}$ remains constant. Hence, the motion of a given agent is uninfluenced by what the other agents' desired distances to the target are, and the team maintains steady and predictable motions; a very suitable quality for the addressed task.

Remark 1: Notice from (12) that, since $\mathbf{R}$ is constant when assumption A1 holds, we can define a constant matrix $\mathbf{A_f} = \mathbf{C}^T\mathbf{C_s}\mathbf{R}^T$ such that:

$$\dot{\mathbf{A}} = -K_c(\mathbf{A} - \mathbf{A_f}). \tag{20}$$

That is, $\mathbf{A}$ converges exponentially to $\mathbf{A_f}$. We can safely assume $\mathbf{A}$ satisfies A1 at the start of the execution. As there are no exact symmetries and alignments of the robots in the desired configuration –as commented in Section II–, we can see that $\mathbf{C}^T\mathbf{C_s}$ satisfies A1, and so does $\mathbf{A_f}$. Hence, $\mathbf{A}$ is exponentially attracted by a configuration that satisfies A1. This justifies disregarding, as we did at the beginning of the section, the degenerate cases. Alternatively, an almost-global stability result could be enunciated, if these cases were contemplated. Note also that the proposed method can be equally applied if the robots and target lie in 2D space. □

We define the *central point of observation* for the current agent positions as the following *weighted centroid*:

$$\mathbf{p_{wq}} = \frac{\sum_{i=1}^{N} s_i^{-1}\mathbf{q_i}}{\sum_{i=1}^{N} s_i^{-1}}. \tag{21}$$

One can see that when the agent positions satisfy the desired viewing angles condition (3) with scales s_i relative to a certain point in space, then that point is equal to $\mathbf{p_{wq}}$. We use next the dynamic behavior of this point to analyze the formation and tracking properties of the proposed controller.

Proposition 1: Under the controller (7) and if A1 is satisfied, the agents converge exponentially to a configuration in which the desired relative viewing angles, and the individual selected desired distances, are achieved with respect to the time-varying weighted centroid of the team.

Proof: Let us express as follows, from (7), the dynamics of the relative position between two robots i and j:

$$\begin{aligned}\dot{\mathbf{q}}_{\mathbf{ij}} = \dot{\mathbf{q}}_{\mathbf{i}} - \dot{\mathbf{q}}_{\mathbf{j}} = K_c(\mathbf{q_{ti}} - \mathbf{R}\mathbf{c^s_{ti}})\\ - K_c(\mathbf{q_{tj}} - \mathbf{R}\mathbf{c^s_{tj}}) = -K_c(\mathbf{q_{ij}} - \mathbf{R}(s_j\mathbf{c_{tj}} - s_i\mathbf{c_{ti}})).\end{aligned} \tag{22}$$

Due to Theorem 1, $\mathbf{R}$ is constant along time, and as the control scales are constant too, the final term of (22) is

a constant, which directly allows to conclude exponential convergence of each position vector $\mathbf{q_{ij}}$ to a vector $\mathbf{q^f_{ij}} = \mathbf{R}(s_j\mathbf{c_{tj}} - s_i\mathbf{c_{ti}})$. We can now define $\mathbf{p_{wq^f}} = \mathbf{q^f_i} + \mathbf{R}(s_i\mathbf{c_{ti}}) = \mathbf{q^f_j} + \mathbf{R}(s_j\mathbf{c_{tj}})$. By isolating in these expressions $\mathbf{q^f_i}$ and substituting, for all i, in (21), one can see that $\mathbf{p_{wq^f}}$ is the weighted centroid of the final robot positions. Then, as $\mathbf{q^f_i} = \mathbf{p_{wq^f}} + \mathbf{R}s_i\mathbf{c_{it}}$ and an analogous expression holds for all other robots, by considering (3) and Section III-B the stated result can be directly concluded. ■

Proposition 2: Under the controller (7) and if A1 holds, the weighted centroid of the agent positions tracks the target's position at all times, and all the agents' velocities align exponentially with the velocity of the weighted centroid.

Proof: The dynamics of the weighted centroid are:

$$\dot{\mathbf{p}}_{\mathbf{wq}} = \frac{\sum_{i=1}^{N} s_i^{-1}\dot{\mathbf{q}}_{\mathbf{i}}}{\sum_{i=1}^{N} s_i^{-1}} = \frac{\sum_{i=1}^{N} s_i^{-1}K_c(\mathbf{q_{ti}} - s_i\mathbf{R}\mathbf{c_{ti}})}{\sum_{i=1}^{N} s_i^{-1}}$$
$$= K_c\frac{(\sum_{i=1}^{N} s_i^{-1})\mathbf{q_t} - \sum_{i=1}^{N} s_i^{-1}\mathbf{q_i} - \mathbf{R}\sum_{i=1}^{N}\mathbf{c_{ti}}}{\sum_{i=1}^{N} s_i^{-1}}. \quad (23)$$

Recalling that $\sum_{i=1}^{N}\mathbf{c_{ti}} = \mathbf{0}$ –due to the target being in the centroid of the default pattern–, we directly reach:

$$\dot{\mathbf{p}}_{\mathbf{wq}} = K_c(\mathbf{q_t} - \mathbf{p_{wq}}), \quad (24)$$

that is, the weighted centroid tracks the target. In addition, as each robot's position converges exponentially to a constant position measured from the variable weighted centroid (Proposition 1), every one of the robots' velocities eventually converges to the velocity of the weighted centroid. ■

The interest of this result is that the central point of observation, i.e., the point which the multirobot team will eventually view with the desired set of relative observation angles, tracks the target at all times with the proposed controller, even when the interagent formation has yet to be reached. This is a behavior one would desire for the proposed target enclosing system.

V. Simulations

This section describes two simulation tests carried out to illustrate the performance of the presented method. In the first one, we used a team of six agents and selected a regular octahedron as default configuration. The chosen values of the control scales s_i for the six robots were: $[1.33\ \ 1.81\ \ 0.78\ \ 0.85\ \ 1.65\ \ 2.11]$. The target's motion was generated by sinusoidal functions. Figure 2 illustrates the results. We can measure the total error in the relative viewing angles of the weighted centroid, with respect to the desired ones, by the following function:

$$e_a = \sum_i \sum_j |\beta_{ij} - \alpha_{ij}|, \quad (25)$$

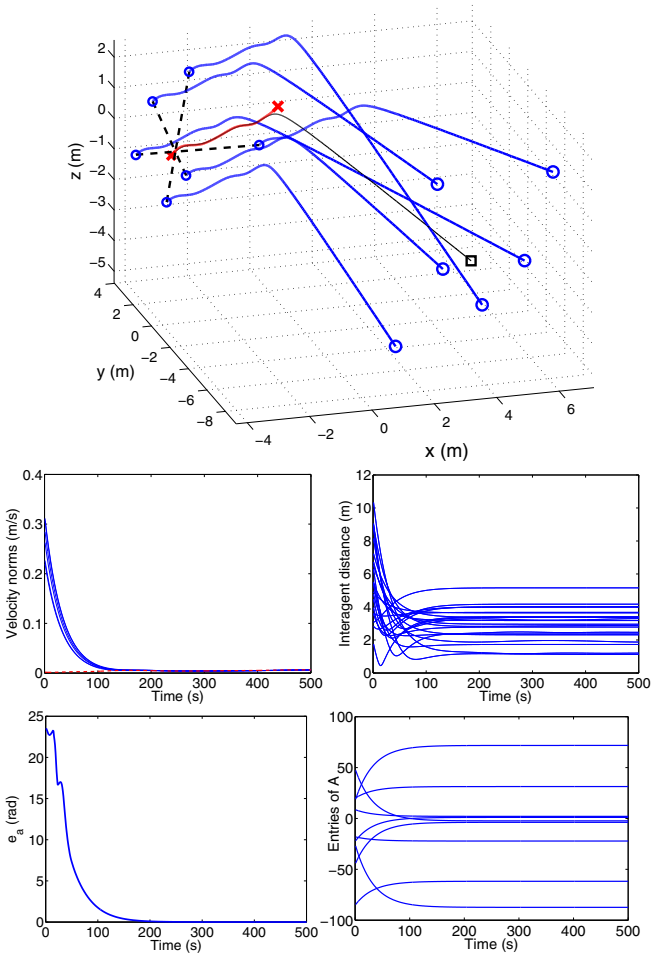

Fig. 2. Simulation results for six-robot example. Top: Paths followed, showing the agents' initial (large circles), and final (smaller circles) positions, and target's initial (large cross) and final (smaller cross) positions. Dashed lines join each agent and the final weighted centroid, whose initial position is also marked (square). Second row: Norms of the robots' and target –in dashed line– velocities (left) and pairwise distances between elements (right). Bottom: Angular error function (left) and entries of $\mathbf{A}$ (right).

where the sums are over all N agents. As can be seen, this error vanishes fast, and the observation and tracking of the target is performed in a steady manner, with a constant $\mathbf{R}$. The robots enclose the target quickly, thanks to the optimality of the rotation matrix used. A set of viewpoints lying in three perpendicular axes, as dictated by the geometry of the octahedron, is exponentially reached. The weighted centroid closely tracks the target's position. The convergence behavior of matrix $\mathbf{A}$ is also shown.

For the second example –illustrated in Fig. 3–, we chose a team of four agents and a regular tetrahedron as default configuration. The target's velocity was again a sum of sinusoids. This time, we added Gaussian noise to the relative position measurements used by the agents, to test the robustness of the method. In addition, the control scales were changed at certain instants during execution. By comparing the intermediate and final team configurations, one can appreciate that the pattern rotation does not change noticeably despite the noise and the scale changes taking place. The steadiness of

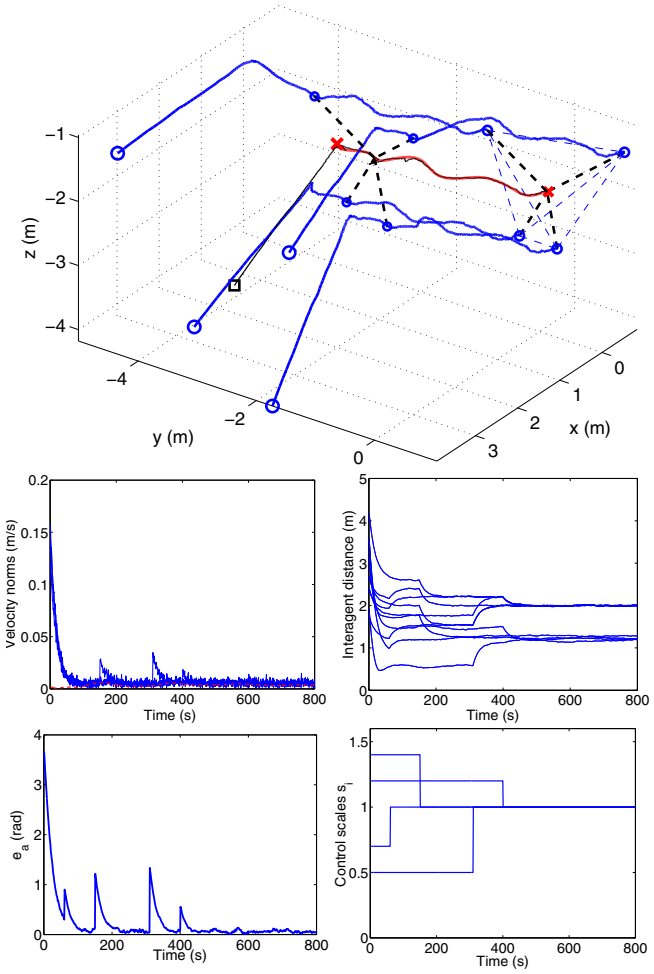

Fig. 3. Results for the four-robot example. Top: Paths followed, showing agents' initial (large circles), and intermediate –at t=280 s.– and final (smaller circles) positions, and target's initial (large cross) and final (smaller cross) positions. Dashed lines join each agent and the intermediate and final weighted centroid, whose initial position is marked (square). Final robot positions are joined by dashed lines. Second row: Norms of the robots' and target –in dashed line– velocities (left) and pairwise distances between elements (right). Bottom: Angular error function (left) and scales s_i (right).

the robots' relative motions is also illustrated by the evolution of the distances between the system's elements (i.e., robots and target). With the piecewise-constant control scales used in this example, the expected convergence behavior occurs within each time interval in which the scales remain constant. Since all control scales become one eventually, the final pattern the agents pursue is the default one: their final positions are very close to forming a regular tetrahedron, while their centroid tracks the target.

VI. Conclusion

We have described a novel method to enclose a moving target in 3D space with a team of robots in order to observe it. Notable points about this strategy are that it can operate on local coordinates and it retains steadiness of agent motions while allowing free individual selections of the robots' distances to the target. Future work can include adapting the framework to tasks that require interaction with physical objects or human agents, and formally studying robustness to disturbance and collision avoidance.

References

[1] G. Guerra-Filho, "Optical motion capture: Theory and implementation," *Journal of Theoretical and Applied Informatics*, vol. 12, no. 2, pp. 61–89, 2005.

[2] C. Robin and S. Lacroix, "Multi-robot target detection and tracking: taxonomy and survey," *Autonomous Robots*, vol. 40, no. 4, pp. 729–760, 2016.

[3] S. Martínez and F. Bullo, "Optimal sensor placement and motion coordination for target tracking," *Automatica*, vol. 42, no. 4, pp. 661–668, 2006.

[4] K. Zhou and S. I. Roumeliotis, "Multirobot active target tracking with combinations of relative observations," *IEEE Transactions on Robotics*, vol. 27 (4), pp. 678–695, 2011.

[5] A. N. Bishop, B. Fidan, B. D. O. Anderson, K. Doganay, and P. N. Pathirana, "Optimality analysis of sensor-target localization geometries," *Automatica*, vol. 46, no. 3, pp. 479–492, 2010.

[6] S. Zhao, B. M. Chen, and T. H. Lee, "Optimal sensor placement for target localisation and tracking in 2D and 3D," *International Journal of Control*, vol. 86, no. 10, pp. 1687–1704, 2013.

[7] K. Hausman, J. Müller, A. Hariharan, N. Ayanian, and G. S. Sukhatme, "Cooperative multi-robot control for target tracking with onboard sensing," *The International Journal of Robotics Research*, vol. 34, no. 13, pp. 1660–1677, 2015.

[8] K.-K. Oh, M.-C. Park, and H.-S. Ahn, "A survey of multi-agent formation control," *Automatica*, vol. 53, pp. 424–440, 2015.

[9] D. V. Dimarogonas and K. J. Kyriakopoulos, "A connection between formation infeasibility and velocity alignment in kinematic multi-agent systems," *Automatica*, vol. 44, no. 10, pp. 2648–2654, 2008.

[10] L. Krick, M. E. Broucke, and B. A. Francis, "Stabilisation of infinitesimally rigid formations of multi-robot networks," *International Journal of Control*, vol. 82, no. 3, pp. 423–439, 2009.

[11] Z. Lin, L. Wang, Z. Han, and M. Fu, "A graph Laplacian approach to coordinate-free formation stabilization for directed networks," *IEEE Trans. on Automatic Control*, vol. 61, no. 5, pp. 1269–1280, 2016.

[12] H. García de Marina, M. Cao, and B. Jayawardhana, "Controlling rigid formations of mobile agents under inconsistent measurements," *IEEE Transactions on Robotics*, vol. 31, no. 1, pp. 31–39, 2015.

[13] S. Zhao and D. Zelazo, "Bearing rigidity and almost global bearing-only formation stabilization," *IEEE Transactions on Automatic Control*, vol. 61, no. 5, pp. 1255–1268, 2016.

[14] S. Ramazani, R. Selmic, and M. de Queiroz, "Rigidity-based multi-agent layered formation control," *IEEE Transactions on Cybernetics*, vol. 47, no. 8, pp. 1902–1913, 2017.

[15] F. Poiesi and A. Cavallaro, "Distributed vision-based flying cameras to film a moving target," in *IEEE/RSJ Intern. Conf. on Intell. Rob. and Systems*, 2015, pp. 2453–2459.

[16] G. López-Nicolás, M. Aranda, and Y. Mezouar, "Formation of differential-drive vehicles with field-of-view constraints for enclosing a moving target," in *IEEE International Conference on Robotics and Automation*, 2017, pp. 261–266.

[17] T.-H. Kim and T. Sugie, "Cooperative control for target-capturing task based on a cyclic pursuit strategy," *Automatica*, vol. 43, no. 8, pp. 1426–1431, 2007.

[18] A. Marasco, S. Givigi, and C.-A. Rabbath, "Model predictive control for the dynamic encirclement of a target," in *American Control Conference*, 2012, pp. 2004–2009.

[19] A. Franchi, P. Stegagno, and G. Oriolo, "Decentralized multi-robot encirclement of a 3D target with guaranteed collision avoidance," *Autonomous Robots*, vol. 40, no. 2, pp. 245–265, 2016.

[20] M. Aranda, G. López-Nicolás, C. Sagüés, and M. M. Zavlanos, "Three-dimensional multirobot formation control for target enclosing," in *IEEE/RSJ International Conference on Intelligent Robots and Systems*, 2014, pp. 357–362.

[21] J. C. Gower and G. B. Dijksterhuis, *Procrustes problems*. Oxford University Press, 2004.

[22] W. Kabsch, "A solution for the best rotation to relate two sets of vectors." *Acta Crystallographica*, vol. 32, pp. 922–923, 1976.

[23] K. Kanatani, "Analysis of 3-D rotation fitting," *IEEE Trans. Pattern Anal. Mach. Intell.*, vol. 16, no. 5, pp. 543–549, 1994.